Synthetic Radar Return-based Neural Network for Detecting Breathing Anomaly

Benjamin M. Hardy*, Swagato Mukherjee, and Tarun Chawla
Remcom Inc., State College PA, United States
*Corresponding author, email: benjamin.hardy@remcom.com

***Abstract*—Radar backscatter is an excellent medium for human sensing in diverse environments. Compared to camera-based monitoring, radar provides privacy and is sensitive to chest variations from breathing and the heart beating. A library of breathing patterns with varying rates, inspiration-to-expiration ratios, and amplitudes was used to animate a human CAD model. The breathing models were then imported into *Remcom's* ray tracer to simulate the complex reflected power through time. The reflected phase and corresponding breathing waveforms were used to train a convolutional neural network to predict a breathing pattern from the incoming radar phase. The neural network predicts breathing patterns within 0.8 mm RMSE over 30 seconds of breathing for normal, hypo-ventilation, hyper-apnea, and tachypnea while hyper-ventilation had a slightly higher RMSE of 2.2 mm.**

***Keywords*—Neural Network, Radar, Physical Optics, Human Sensing, Synthetic Radar, Simulation.**

I. Introduction

Radar-based human sensing systems are capable of capturing movement, occupancy, and vital signs in diverse environments [1]. Applications of radar-based vital sign monitoring include sleep apnea diagnosis [2], fall detection [3], through-wall detection [4], and in-cabin sensing [5]. Compared to camera-based systems, radar-based vital sign monitoring is less invasive and provides higher sensitivity to small movements [6]. Challenges of radar-based vital sign monitoring include accounting for random body movements [7], signal separation from individuals [8] , and environmental interference [4]. Radar algorithms are often tested using previously published data sets, chamber measurements, or ad-hoc laboratory setups. There are few data sets that showcase radar returns from humans exhibiting abnormal vital signs [9]. Furthermore, diverse interference sources such as outdoor environments are challenging to emulate in chamber measurements whereas simulation allows customized modeling of realistic scenes providing heterogeneity in datasets. This work builds from previous validation of *Remcom's* ray tracer against semi-anechoic chamber measurements of a 28 GHz radar reflecting from a breathing human [10].

II. Methods

As described in [10], a breathing CAD model was used to generate 200 waveforms with random breathing rates, inspiration-to-expiration (IE) ratios, and amplitudes. Each parameter was uniformly distributed across values corresponding to normal, hyper-ventilation, hypo-ventilation, hyper-apnea, and tachypnea breathing patterns. The breathing rate (BR) was 6 to 50 breaths/min, the amplitude (amp) was 1 to 9 mm, and the IE ratio was 0.15 to 1.1. To mimic random body movements, each breathing waveform had up to 5% random variation in amplitude and up to 20% drift on a per breath basis. Each breathing waveform is 30 s long. A *Blender* script displaced the phantom's chest and stomach vertices according to the 200 breathing waveforms. CAD models were exported and simulated every 100 ms with *Remcom's* 3D ray tracer. The phantom was assigned the relative permittivity of human skin at 28 GHz $\epsilon_r = 15.5 - 14.2j$ according to [11]. The transceiver was assigned a gaussian antenna pattern with an input power of 0 dBm. The transceiver was 2 m away from the human phantom and vertically polarized. Each simulation took approximately 5 seconds. The 200 waveforms and 300 time points resulted in a total of 60,000 simulations. A phase unwrapping algorithm was applied to each returned phase. The waveforms and their respective phases were split between sets of 70% training, 15% testing, and 15% validation cases. Using *TensorFlow*, a convolutional neural network (CNN) was created with the following architecture:

1. 1D convolution with filter = 32, kernel = 3.
2. Max pooling with pool size = 2.
3. 1D convolution with filter = 64, kernel = 3.
4. Linearization and a dense layer of 128 units.

5 additional validation cases were included to demonstrate the network's ability to predict breathing waveforms characteristic of abnormal breathing patterns. Each breathing human model was facing the antenna in a sitting position. To investigate how rotation of the body affects the data, simulations were run with the human model seated and rotated 15° and 30° azimuthally.

III. Results

After training for 252 epochs, the mean squared error for the training and validation was 2.6% and 9.4% respectively. For the 5 representative breathing waveforms in Fig. 1, the root-mean-squared-error (RMSE) was 0.3, 2.2, 0.3, 0.7, 0.2 mm for the normal, hyper-ventilation, hypo-ventilation, hyper-apnea, and tachypnea patterns respectively. Hyper-ventilation's prediction suffered the most since both its amplitude and IE ratio were towards the edge of the training

data set input parameters. In Fig. 2, the returned phase is plotted for 3 rotated human cases. At 0 and 15° the phase is clearly varying on a per breath basis. However, at 30° the reflections from the chest are diminished. The training data was entirely from the 0° case.

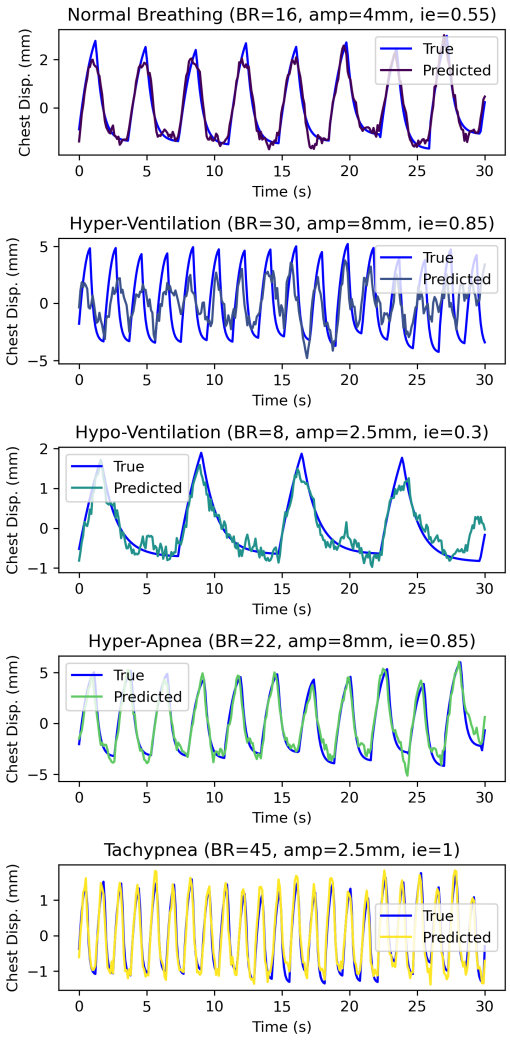

Fig. 1. The true and predicted waveforms for the 5 representative breathing cases. With only 200 sets of phase and breathing waveforms, The CNN predicts normal, hypo-ventilation, hyper-apnea, and tachypnea patterns within 0.8 mm across the 30 seconds of breathing. More waveforms classified as hyper-ventilation would improve the predictions.

IV. Discussion

To improve the predictions, more synthetic data near the edge cases with higher IE ratios and amplitudes are needed. Fig. 1 suggests that for a sitting human, with enough training data, abnormal breathing patterns could successfully be determined as long as the phase of the radar is accessible. Adding noise sources, phantom variation, rotations such as that represented in fig. 2 will allow the model to predict waveforms in more realistic scenarios such as inside a car or in a hospital setting. By augmenting and improving the

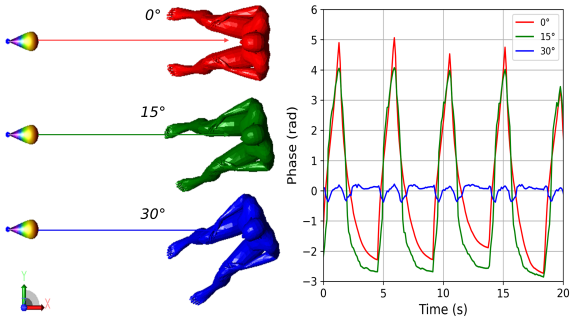

Fig. 2. The phase returned from the human at different rotations. The CNN was only trained for humans at the 0° configuration.

dataset, a dynamic prediction and classification model will be created using a recurrent neural network.

V. Conclusion

In this work, a CNN was designed to predict human breathing waveforms from simulated radar phase from an animated human model. The model predicts breathing patterns within 0.8 mm RMSE over 30 seconds of breathing for normal, hypo-ventilation, hyper-apnea, and tachypnea while hyper-ventilation has a RMSE of 2.2 mm. Further diversification of the data set including rotations, phantom variations, and noise will enhance the model's ability to predict breathing in more realistic environments.

References

[1] Mamady Kebe et al. "Human Vital Signs Detection Methods and Potential Using Radars: A Review". In: *Sensors* 20.5 (2020).

[2] Vinh Phuc Tran et al. "Doppler Radar-Based Non-Contact Health Monitoring for Obstructive Sleep Apnea Diagnosis: A Comprehensive Review". In: *Big Data and Cognitive Computing* 3.1 (2019).

[3] Abhijit Bhattacharya et al. "Deep Learning Radar Design for Breathing and Fall Detection". In: *IEEE Sensors Journal* 20.9 (2020), pp. 5072–5085.

[4] Xiaolin Liang et al. "Ultra-Wideband Impulse Radar Through-Wall Detection of Vital Signs". In: *Scientific Reports* 8.1 (Sept. 2018), p. 13367.

[5] Jin-Kwan Park et al. "Noncontact RF Vital Sign Sensor for Continuous Monitoring of Driver Status". In: *IEEE Transactions on Biomedical Circuits and Systems* 13.3 (2019), pp. 493–502.

[6] Lingyun Ren et al. "Comparison Study of Noncontact Vital Signs Detection Using a Doppler Stepped-Frequency Continuous-Wave Radar and Camera-Based Imaging Photoplethysmography". In: *IEEE Transactions on Microwave Theory and Techniques* 65.9 (2017), pp. 3519–3529.

[7] Changzhi Li et al. "Complex signal demodulation and random body movement cancellation techniques for non-contact vital sign detection". In: *2008 IEEE MTT-S International Microwave Symposium Digest*. 2008, pp. 567–570.

[8] Marco Mercuri et al. "Automatic radar-based 2-D localization exploiting vital signs signatures". In: *Scientific Reports* 12.1 (May 2022), p. 7651.

[9] Sven Schellenberger et al. "A dataset of clinically recorded radar vital signs with synchronised reference sensor signals". In: *Scientific Data* 7.1 (Sept. 2020), p. 291.

[10] Swagato Mukherjee et al. "Animating Vital Signs in Radar Simulations: Comparing Physical Optics Against 28.5 GHz Channel Measurements". In: *2024 IEEE Radar Conference (RadarConf24)*. 2024, pp. 1–5.

[11] T. Wu et al. "The human body and millimeter-wave wireless communication systems: Interactions and implications". In: *IEEE International Conference on Communications (ICC)* (2015).